RADIATION ENVIRONMENT FOR RENDEZVOUS AND DOCKING WITH NUCLEAR ROCKETS

D.R. Rogers, E.A. Warman, B.A. Lindsey

Aerojet Nuclear Systems Company
Sacramento, California

Planning for operations such as rendezvous and docking of a vehicle powered by a nuclear rocket engine with a space station requires consideration of the radiation environment produced by the engine in addition to the natural space radiation environment. This paper provides radiation environment data for the NERVA engine which may be utilized in estimating radiation exposures associated with various space maneuvers. Spatial distributions of neutron and gamma tissue kerma rates produced during full thrust operation of the engine are presented. The corresponding biological dose rates will be due predominantly to neutron contributions except within the region in space which is shadowed by the liquid hydrogen propellant. Forward of the vehicle, dose rates will depend on the characteristics of the propellant module and payload as well as those of the engine and will vary during a mission as propellant is consumed. Final rendezvous with an orbiting space station would be achieved subsequent to full thrust operation during a period of 10 or more hours duration in which impulse is delivered by the propellant used for removal of decay heat. Consequently, post operation radiation levels are of prime importance in estimating space station exposures. Maps of gamma kerma rates around the engine are provided for decay times of 4 and 24 hours after a representative firing. Typical decay curves illustrating the dependence of post operation kerma rates on decay time and operating history are included. Examples of the kerma distributions around the engine which result from integration over specific exposure periods are shown.

This paper summarizes data pertaining to the radiation environment which is produced near the NERVA* engine. The radiation environment during full thrust operation and during post-operation periods has been considered. These are presented in a format intended to make the data useful in considering the radiation exposures associated with rendezvous and docking maneuvers.

The NERVA engine employs a graphite moderated, beryllium reflected reactor which heats and exhausts liquid hydrogen propellant to develop 75,000 lbs thrust. The NERVA flight engine configuration is illustrated in Figure 1. Minimal radiation attenuation is provided for radiation emitted in directions other than along the forward centerline axis. An internal shield is included within the Pressure Vessel and Reactor Assembly (PVARA) to provide protection for critical engine system components. Some potential manned missions may require additional biological shielding. The manned mission shielding requirements depend on the characteristics of the entire nuclear stage, including the propellant module and payload as well as the engine. The engine design has provision for inclusion of an external disk shield at the location indicated in Figure 1, if additional protection is required for manned payloads. The engine is coupled to a propellant module with 300,000 lbs liquid hydrogen capacity. The payload is located forward of the propellant module.

When operating at full thrust, the reactor fission power is a little over 1500 megawatts. The radiation energy which escapes from the system is equivalent to about 1% of the total fission power. Thus, the magnitude of the NERVA engine as a source is such that radiation exposure may be an important consideration in planning rendezvous and docking maneuvers.

NERVA ENGINE WITH DISK SHIELD

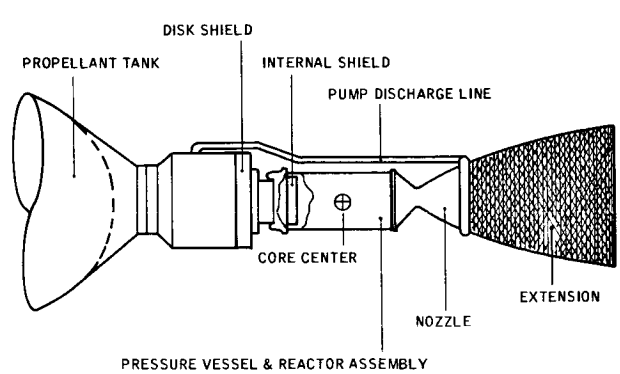

FIGURE 1

* The Nuclear Engine for Rocket Vehicle Application Program (NERVA) is administered by the Space Nuclear Systems Office, a joint office of the USAEC and NASA. Aerojet Nuclear Systems Company is prime contractor for the engine system and Westinghouse Electric Corporation is principal subcontractor responsible for the nuclear subsystem.

I. OPERATING RADIATION ENVIRONMENT

The spatial distribution of gamma radiation emerging from the engine during full power operation is shown in Figure 2. The data shown are iso-KERMA rate contours expressed in units of rads (tissue)/second. These controus provide a pictorial representation of the directional dependence of the intensity of radiation leakage from the engine. It is apparent that there is no strong dependence on direction except in a relatively small cone about the forward axis, due to the effect of the shadow shield in the forward end of the pressure vessel. The highest intensities external to the pressure vessel occur at reactor midplane where the peak value is about 3×10^5 rads/sec in contact with the pressure vessel. The radiation leakage from the PVARA in the aft or nozzle direction is only slightly less than the radial leakage, but the nozzle assembly provides some additional attenuation. In the forward direction, the gamma leakage is reduced by a factor of approximately 30 by the combined effects of the internal shield and the fuel element support plate.

Figure 3 presents the neutron leakage rates at full power conditions. The right half of this figure shows isoflux contours of fast neutrons (energies greater than 0.9 Mev) emerging from the engine in units of neutrons/cm^2-sec. The left half of the figure contains contours of KERMA rate resulting from neutrons of all energies in units of rads(tissue) per second. In the case of neutrons, intensities in the aft direction are slightly higher than to the side, because the beryllium reflector shields more effectively against neutrons than against gamma rays. The dependence of neutron leakage on direction is not strong except within the region of influence of the internal shield. If the neutron KERMA rates are compared with gamma KERMA rates of Figure 2, it is apparent that the tissue KERMA rate due to neutrons is as high or higher than that due to gamma rays at all locations. Hence, in biological dose considerations, in which the biological effectiveness of the radiation must be considered, the neutron contribution will clearly dominate. Reduction of biological dose rates through means other than distance (i.e., by shielding) is a combined neutron and gamma shielding problem. However, it is important to point out that the liquid hydrogen in the propellant tank provides a tremendous indigenous neutron shielding effect. As a result, almost all of the dose to the payload is due to gamma radiation.

Figure 2

GAMMA KERMA RATES NEAR ENGINE AT FULL POWER
UNITS: RADS(TISSUE)/SECOND

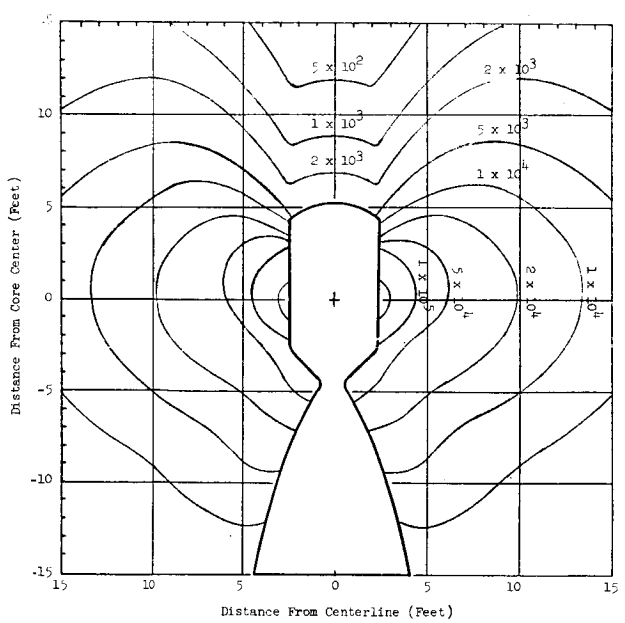

Figure 3

NEUTRON FLUXES AND KERMA RATES NEAR ENGINE AT FULL POWER

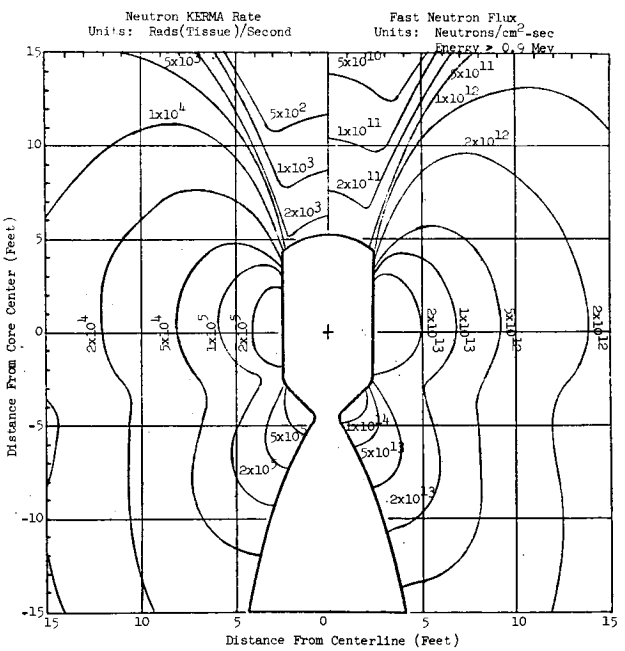

The full power operating gamma radiation environment is extended in the gamma KERMA rate map of Figure 4 to distances of approximately 200 ft from the reactor center. The Nuclear Flight Propulsion Module (NFPM) depicted in this figure includes a 33-ft diameter propellant tank with 15° half-angle conical tank bottom. These data were calculated for a minimum shield configuration; i.e., no external disk shield was included. Furthermore, the contours near the forward axis do not include any attenuation by the propellant module or payload. The actual intensities within the fairly narrow cone influenced by the propellant module will vary during the mission, increasing as the mass of liquid hydrogen remaining in the propellant tank decreases. The contours shown are representative of the limit approached as the liquid hydrogen nears total depletion at the end of the last firing. Consequently, they represent worst case limits for gamma KERMA rates experienced during a nose-on approach.

Figure 4

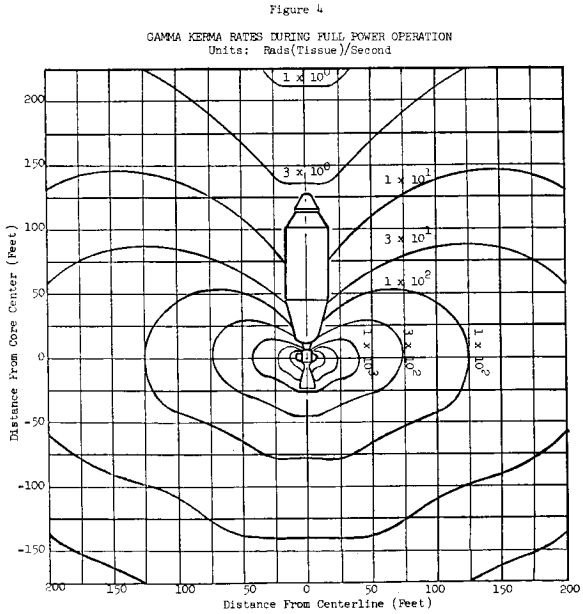

A corresponding neutron map covering the same spatial region as Figure 4 is shown in Figure 5. The fast neutron intensities were obtained with the same assumptions: the minimum shield configuration with no attenuation in regions external to the PVARA. In the area shadowed by the propellant module, this places a quite conservative upper limit on the neutron KERMA rate, because the liquid hydrogen is such an effective shield against neutrons. Even at end of burn, the liquid hydrogen required for cooldown plus the hydrogen vapor in the tank are sufficient to reduce the neutron KERMA rate to a relatively insignificant level.

Figure 5

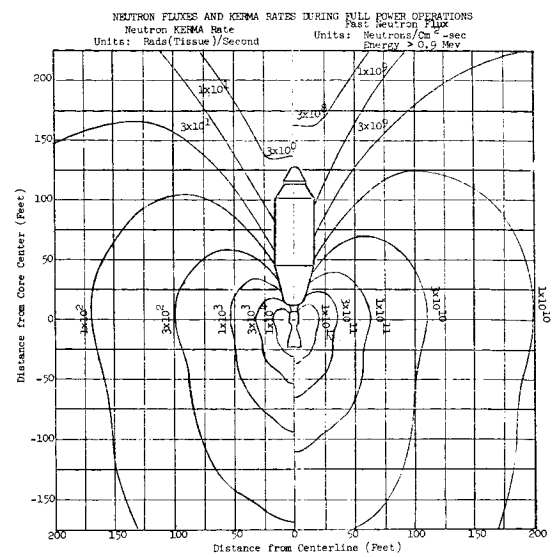

Extensive calculation of tank-top gamma KERMA rates have been performed for the reference 300,000 lb capacity 15° propellant tank, with various liquid hydrogen levels in the tank. In Figure 6, the results of some of these calculations for a point on centerline at the top of this tank are plotted as a function of residual propellant mass. The neutron KERMA rate at this location varies very rapidly with the mass of liquid hydrogen and is significant only when the tank is almost entirely drained. Since approximately five thousand pounds of liquid hydrogen are required for cooldown after the last burn, the neutron exposure above tank top is negligible compared to the gamma exposure. This is true only for the fairly narrow cone in space which is shadowed by the propellant tank.

The KERMA rates expected along the forward centerline axis can be seen to vary through about three decades depending on how much propellant is in the tank. Thus, during most of a mission, the on-axis KERMA rate is much less than the KERMA rate at the end of the last burn. As an example, the tank top KERMA rates occurring at the end of each of four burns of a typical mission (unmanned) reusable interorbit ferry) are indicated in Figure 6. The KERMA rate during a nose-on approach following the second burn is about a factor of 10 lower than for such an approach after the fourth burn. In a manned mission which includes a biological shield at the engine, the on-axis KERMA rates will, of course, be further reduced. A typical 10,000 lb disk shield at the engine would reduce the tank top KERMA rate by about a factor of 20 during most of a mission. Near the end of the last burn, when line-of-sight contributions to the tank top KERMA rate are more important relative to contributions from scattering in the propellant, the effective attenuation factor would increase somewhat. Again, the on-axis environment pertains only in a fairly narrow cone and increases rapidly toward side leakage values as the detector location moves out of the influence of the tank and/or the protection of the disk shield.

Figure 6

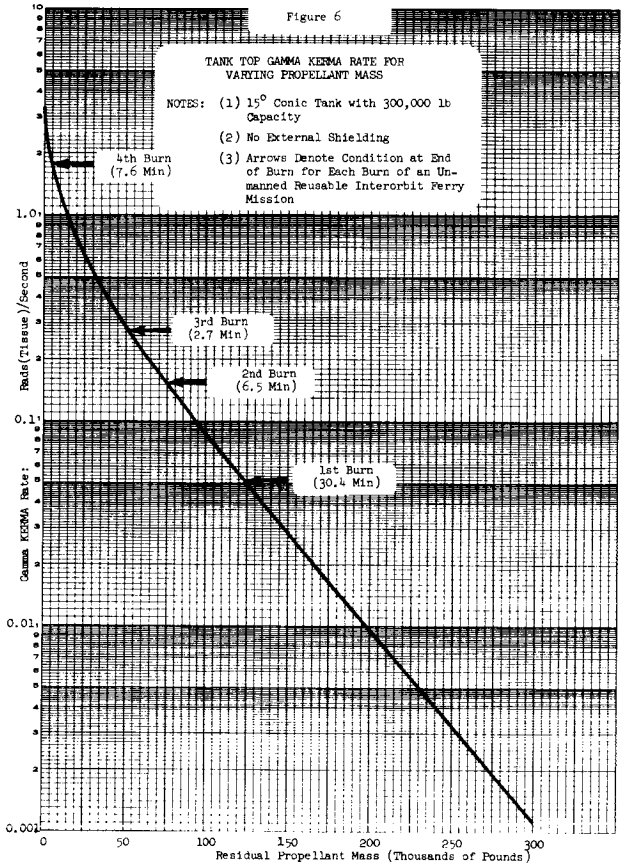

Figure 7

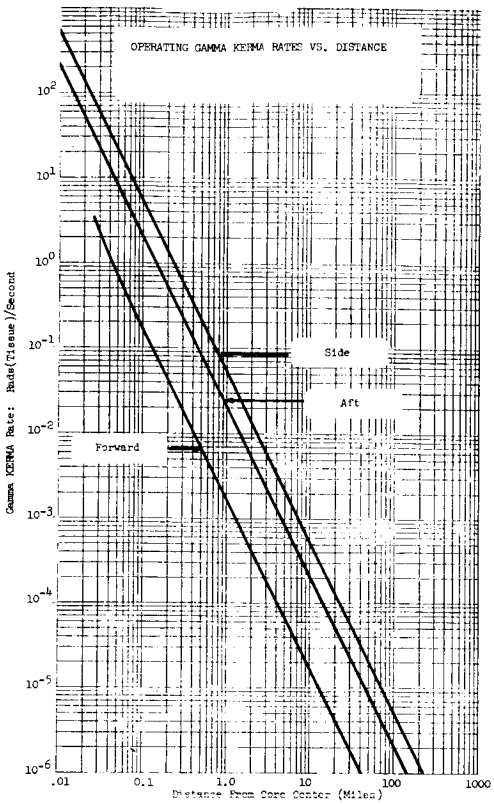

The data from the extremities of Figures 4 and 5 may be extrapolated with little error by inverse r^2 from the engine to obtain estimates of KERMA rates at greater distances. Figure 7 illustrates the $1/r^2$ extrapolation of side and aft gamma leakage data from Figure 4 out to distances of 100 miles from the engine. At 1 mile to the side, the gamma KERMA rate has dropped to 5×10^{-2} rads(tissue)/sec and at 100 miles is only 5×10^{-6} rads(tissue)/sec. The data shown for the forward direction was extrapolated from the dose rate at tank top (126 feet from reactor center) with no residual hydrogen. No payload attenuation or disk shield is included.

Extrapolated neutron KERMA rates are plotted in Figure 8. The neutron KERMA rate at 1 mile ranges from 3×10^{-1} rads(tissue)/sec in the aft direction to 1×10^{-1} rads(tissue)/sec at the side. These fall to 3×10^{-5} and 1×10^{-5} rads (tissue)/sec, respectively, at 100 miles.

Figure 8

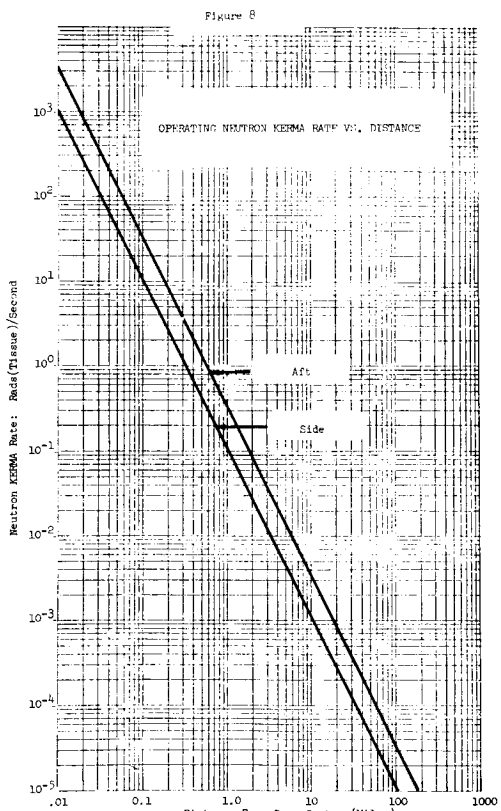

II. SHUTDOWN RADIATION ENVIRONMENT

In lunar shuttle missions, full power operation would ordinarily terminate anywhere from a hundred to several hundred miles from the space station. The subsequent maneuvering to close the distance with the station would be performed using the impulse delivered by the propellant used for afterheat cooldown. Final docking would occur after most of the cooldown impulse has been expended. This would be at least 10 hours after shutdown. The problem of estimating space station exposures during rendezvous and docking, therefore, primarily involves the post-operation radiation environment.

The magnitude of the gamma source in the engine drops rapidly after shutdown, but remains quite significant in terms of biological dose rates in the vicinity of the engine. The fission product source strength and resulting gamma intensities external to the engine are quite dependent on time after shutdown and the operating history. Post-shutdown gamma KERMA rates have been examined for representative periods of operation and decay. Figure 9 contains gamma iso-KERMA rate contours near the engine which are based on a 30-min continuous full-power firing. The data shown on the left half of the figure are KERMA rates calculated for a decay time of 4 hours after the 30-min firing. KERMA rates after an additional 20 hours or a total of 24 hours decay shown for comparison on the right half of the figure. Only gamma KERMA rates are significant because the photoneutron production in beryllium after shutdown is insufficient to result in neutron intensities which compete with the gamma rays.

FIGURE 9

GAMMA KERMA RATES NEAR ENGINE FOLLOWING 30 MINUTE FULL POWER FIRING
Units: Rads(Tissue)/Second

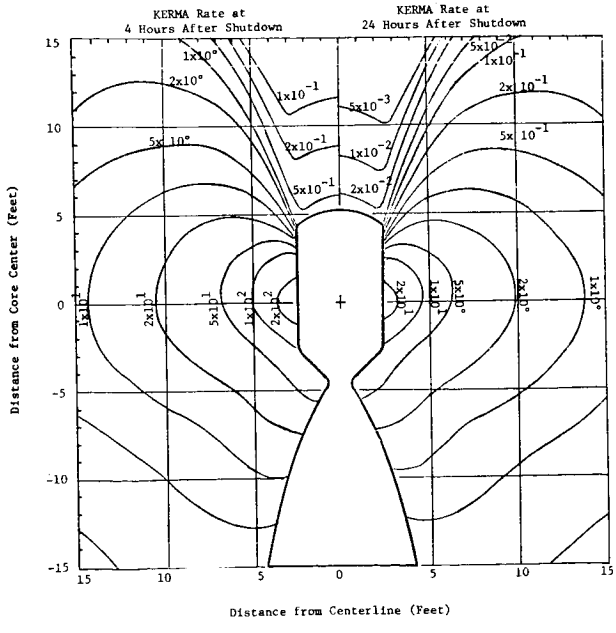

The gamma KERMA rate maps for 4 hours and 24 hours after a 30-min firing have been extended in Figure 10 to cover an area which encompasses the entire vehicle. These contours are for a minimum shield configuration (internal shield only). The levels near the forward axis do not include any propellant module or payload effects.

At 4 hours after shutdown, the KERMA rate 100 ft to the side is 1.7 x 10^{-1} rad/sec and this decays to 1.5 x 10^{-2} rad/sec at 24 hours after shutdown. On the forward axis, in the shadow of the internal shield, the KERMA rate is about 2 decades lower.

FIGURE 10

GAMMA KERMA RATES FOLLOWING 30 MINUTE FULL POWER FIRING
Units: Rads(Tissue)/Second
KERMA Rate at
4 Hours After Shutdown
Gamma KERMA Rate at
24 Hours After Shutdown

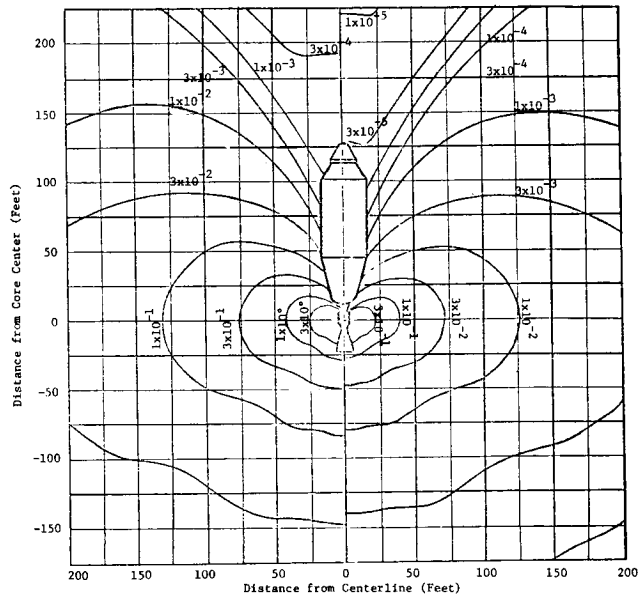

For distances beyond those covered in the previous map, the data may be extrapolated by inverse r^2. This extrapolation is shown for the forward, side, and aft directions from the engine in Figure 11 for distances out to 100 miles. At 1 mile to the side, the KERMA rate is about 5 x 10^{-6} rads (tissue)/sec at 24 hours after shutdown.

Figure 11

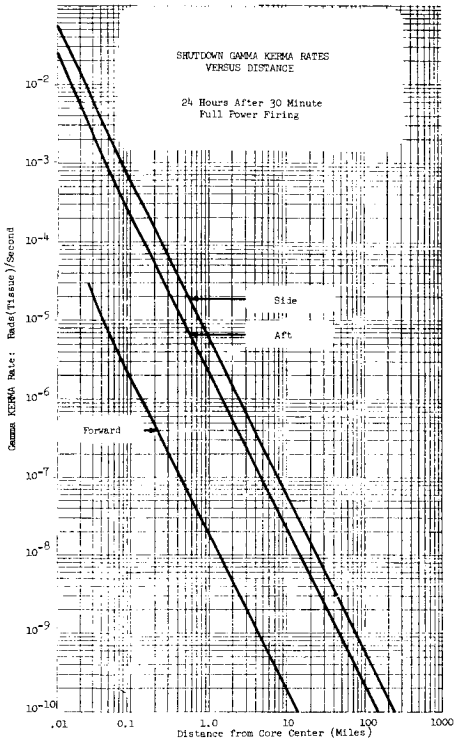

Figure 12

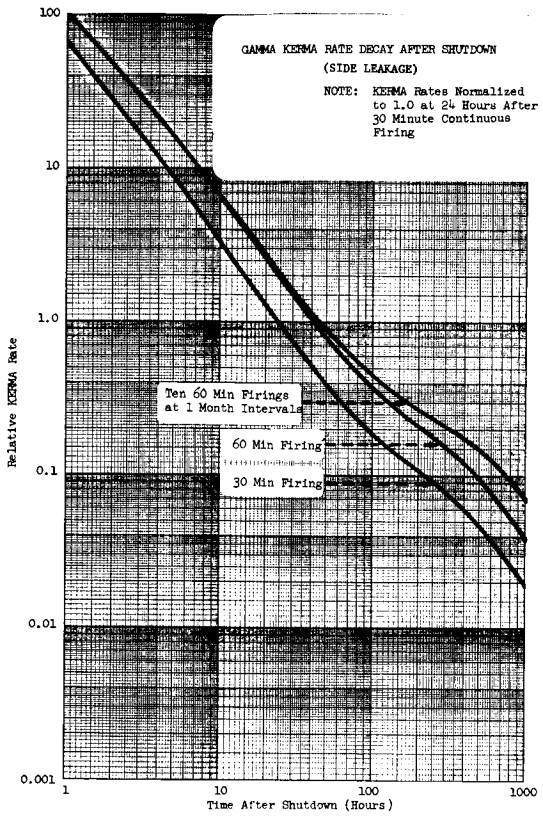

The data of Figure 12 illustrate the dependence of KERMA rate on time after shutdown for representative operating histories. The data are normalized such that the KERMA rate 24 hours after a 30-min burn is 1.0. Thus, KERMA rate data of Figures 9, 10, and 11 for 24 hours decay may be scaled to other operating and decay conditions. For example, at 100 ft to the side of the engine, the KERMA rate 1 hour after a 30-min firing is a factor of 65 greater than the KERMA rate at 24 hours or approximately 1.0 rads (tissue)/second. In Figure 12, the KERMA rates after a 30-min burn are compared with those after a 60-min burn and those following a sequence of ten 60-min operations. The latter represents the total rated lifetime of an engine. KERMA rates for other burns can be scaled from the data for 30 minutes at full power in direct proportion to the power integral for the burn so long as the decay time is long compared to the burn time.

Cumulative radiation exposures may be obtained by integrating the KERMA rate versus time curve over the exposure duration. Iso-KERMA contours around the engine are shown in Figure 13 for exposures which would be accumulated during the periods from 4 hours to 30 days after shutdown and from 24 hours to 30 days after shutdown following a 30-min burn. These might represent exposures resulting during a 30-day docking, starting at 4 hours or 24 hours after termination of the firing. Data for the minimum shield configuration, consistent with Figure 10.

FIGURE 13

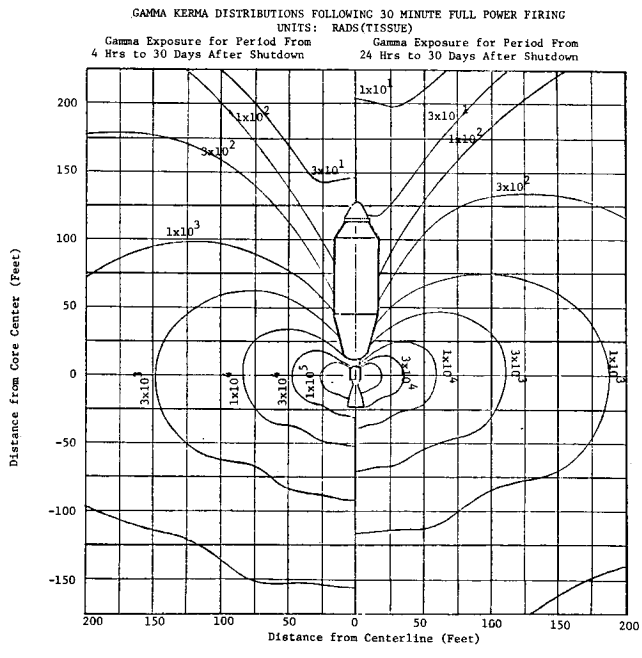

III. SUMMARY

In summary, the operating and shutdown radiation environment in the vicinity of the NERVA engine is presented in such a manner as to facilitate calculations of accumulated dose for rendezvous and docking maneuvers. The units of tissue rads/sec were chosen for two reasons: (1) the dose due to the stay time at any one point in traversing these maps would probably be best calculated from a per second value, and (2) the use of the tissue rad value permits one to proceed at the present maturity of mission planning by simply assuming a single conversion to rem dose based on an assumed quality factor. These data are tissue KERMA values, with no attempt to compute secondary radiation contributions in the tissue. Much larger uncertainties in radiation levels are associated with the design evaluation of a flight engine than those introduced by assumptions normally made in KERMA to dose conversion calculations.

The preponderance of the neutron levels during operation should be pointed out. If an average conversion from Rad(T) to Rem were to be based on an RBE of 7, the Rem dose from neutrons would eclipse that from gamma radiation in all but the forward direction (i.e., the region affected by the presence of the liquid hydrogen propellant tank).

Use of these data in detailed planning for specific missions will have to take into account the indigenous shielding and secondary gamma production in the approaching vehicle, while the NERVA engine is operating, and the indigenous shielding for the relatively soft gamma radiation after shutdown. For a first approximation, the operating radiation environment at less than full thrust would be in direct proportion to the full power/partial power thrust levels.

An "approach corridor" concept could be adopted in which access and egress to and from the shutdown NERVA engine would be made along the propellant tank within a band of a few feet from the tank outer surface. This would allow approach from the payload vicinity for maintenance in the tank bottom vicinity with possibly no additional shielding over and above the engine disk shield provided the stay time is very short and a combination of engine operating time and decay time did not result in prohibitively high radiation levels.

Remotely operated equipment (such as teleoperators) would be required for maintenance of most, if not all, portion of the engine, except after only short durations of operation at full power.

Cumulative exposure calculations for specific rendezvous and docking maneuvers have not been attempted herein, but enough data have been provided to allow this to be done in a relatively straight forward manner, as the details of such maneuvers with NERVA are developed.